Polymer 51 (2010) 1771–1778

Contents lists available at ScienceDirect

Polymer

journal homepage: www.elsevier.com/locate/polymer

Nanoscale patterning through self-assembly of hydrophilic block copolymers with one chain end constrained to surface

Xiang Gao [1], Shiping Zhu*, Heather Sheardown, John L. Brash

Department of Chemical Engineering, McMaster University Hamilton, ON, Canada L8S 4L7

ARTICLE INFO

Article history:
Received 14 December 2009
Received in revised form
7 February 2010
Accepted 13 February 2010
Available online 18 February 2010

Keywords:
Nanopatterning
Polymer brush
Hydrophilic block copolymer

ABSTRACT

Poly(oligo(ethylene glycol) methacrylate) (POEGMA)-block-poly(2-(methacryloyloxy) ethyl trimethylammonium chloride) (PMETAC) brushes were synthesized on silicon wafer surfaces by a surface-initiated atom transfer radical polymerization (ATRP) method. Salt-triggered collapse of the polyelectrolyte in solution was employed to induce phase segregations between the two hydrophilic blocks and thus to develop nanoscale patterns. The smallest feature size was about 10 nm and was tunable on the nanoscale. Various patterns including spherical aggregates, wormlike aggregates, and line patterns were obtained through adjusting the upper block layer thickness. These nanopatterns could switch between the different morphologies through the treatment of selective solvents. The adsorption behavior of fibrinogen on these patterns was also studied by ellipsometry, water contact angle measurement, AFM and radio labelling method. The results showed that these nanopatterns possess the ability to pattern proteins.

© 2010 Elsevier Ltd. All rights reserved.

1. Introduction

Over the past decades, nanotechnology has been generating significant interest in various fields. In biological and medical areas, nanopatterns hold the ability to pattern proteins, cells or DNAs [1–5]. These patterns have found great values in a variety of applications, for example, in the preparation of bio-microelectromechanical systems, biochips, microfluid devices, biosensors, biodiagnostic devices etc. [6–12]. In biological fundamental studies, the nanostructure has helped biologists to investigate behaviors of individual biomolecules by isolating and giving them specific surroundings [13,14].

Fabrication of nanopatterns can be divided into “top-down” and “bottom-up” methods [15,16]. The “top-down” lithographic method is well established and frequently used. It can produce high quality nanopatterns with arbitrary designs at a nanoscale precision. However, when the feature sizes less than 100 nm are required, the complex procedures associated with electron-beam or certain probe tips including dip-pens bear high costs [7,16]. The “bottom-up” method makes full use of self-assembly of various materials to produce nanoscale patterns at low costs [16]. It has an obvious advantage when large area periodic nanopatterns are targeted.

The self-assembly of block copolymers has been widely employed to generate nanoscale patterns in the size range below 100 nm [15,17,18]. In the recent years, several studies were carried out to self-assemble block copolymer brushes into nanoscale patterned surfaces [19–24]. These copolymer brushes are chemically grafted on various surfaces. The chemically grafted polymer chains through covalent bonds on the surfaces can lead to stable patterned surfaces, overcoming some problems associated with spun-cast films due to solubility or swelling. The recent development of various surface-initiated living polymerization techniques offers precise design for copolymer brushes on surface. Furthermore, these living polymerization methods yield polymer brushes with active chain ends. They can be readily modified to introduce more functions to the surface (e.g. biofunction or specific adsorption capacity).

Zhao and Brittain et al. [25] demonstrated the feasibility of introducing nanoscale patterns by self-assembly of tethered polystyrene-b-poly(methyl methacrylate) brushes after some treatment of selective solvents. Genzer and Ruhe et al. [26–30] showed that, by varying chain lengths of the blocks, different surface morphologies including flat, micellar and bicontinuous morphologies could be achieved. In Choi et al.'s work, the solvent treatments were found to affect surface morphologies as well [31]. Bruening and Baker et al. [32] prepared amphiphilic triblock copolymer brushes on surface and achieved more uniform domain sizes. In our previous work [33], we introduced various nanopatterns to surface through self-assembly of grafted

* Corresponding author. Tel.: +1 905 525 9140x24962; fax: +1 905 521 1350.
E-mail address: zhuship@mcmaster.ca (S. Zhu).
[1] Present address: Department of Chemical and Biological Engineering, Zhejiang University, Hangzhou, China 310027.

0032-3861/$ – see front matter © 2010 Elsevier Ltd. All rights reserved.
doi:10.1016/j.polymer.2010.02.021

poly(oligo(ethylene glycol) methacrylate) (POEGMA)-block-poly (methyl methacrylate) (PMMA) brushes. Simple water treatments induced phase segregations of the POEGMA and PMMA segments and thus generated the nanoscale patterns. The smallest feature size was less than 10 nm. Various patterns including spherical aggregates, wormlike aggregates, line patterns, perforated layers and complete overlayers were obtained by varying the upper block layer thickness. These patterns possessed some unique stimuli-responsive properties and were switchable between the different morphologies with simple solvent treatments. All these studies showed that the self-assembly of block copolymer brushes represents a promising approach for the preparation of nanoscale patterns on surface.

The objective of this work is to prepare nanoscale patterns by self-assembly of block copolymer brushes to pattern biomolecules for potential biological and medical applications. One basic requirement for these nanopatterns is that their interfaces must have both binding capacity for targeted biomolecules and at the same time a non-fouling background which resists non-specific adsorption of proteins or cells. POEGMA is chosen in this work to provide a non-fouling background. PEG-based polymers are the most important type of materials that provide non-biofouling functions because of their excellent resistance to non-specific protein adsorption and cell adhesion [34–38], as well as their non-toxic and non-immunogenic properties [6,35]. Various patterned PEG-based surfaces have been prepared to pattern proteins [39–44] or cells [35,37,43,45–50] for different applications. A hydrophobic polymer has always been used as the top block, to assure phase segregation. In our previous work, PMMA was used as the hydrophobic top block for the phase separation [33]. Hydrophobic polymers have ability to adsorb proteins non-selectively. The patterns prepared from this design have potential to pattern biomolecules with limited bioapplications. Although a hydrophobic surface can adsorb proteins, it has been found that some adsorbed proteins on surface experience significant change in conformation and as a result, lose their bioactivities. Besides, the non-selectivity of hydrophobic surfaces also makes it challenging in further modification of chain ends for selectively capture of targeted biomolecules.

The use of hydrophilic polymer as the top block could provide an ideal solution to this problem. However, the difficulty lies in that phase segregation between two hydrophilic blocks cannot be induced by simple water treatment. The approach in the current work is to use a polyelectrolyte as the top block. In salt solution, the polyelectrolyte chains collapse and form patterns on the surface. Furthermore, the static electrolyte charges may bring more advantages, e.g. external electric field may be applied to control the formation of patterns. The objective of this work is therefore to prepare the nanoscale patterns from block copolymer brushes having two hydrophilic segments by salt solution treatment and to explore ability of the polymer patterned surface in developing protein patterns.

2. Experimental section

2.1. Materials

$Cu^{I}Br$ (99.999%), $Cu^{I}Cl$ (99.99%), $Cu^{II}Cl_2$ (99.995%), 2,2′-bipyridyl (Bipy) (99%), ethyl α-bromoisobutyrate (EBIB) (98%), and methanol (HPLC grade, Aldrich) were purchased from Aldrich and used as received. Oligo(ethylene glycol) methacrylate (OEGMA) (98%, $M_n = 300$ g/mol, Aldrich) was distilled over CaH_2 under vacuum. [2-(Methacryloyloxy)ethyl] trimethylammonium chloride (METAC) solution (75 wt% in H_2O, $M_n = 207.70$ g/mol, Aldrich) was passed through an inhibitor remover column (Aldrich) to remove the inhibitor, monomethyl ether hydroquinone. Toluene (HPLC grade, Aldrich) was distilled over CaH_2 twice. Deionized water from the Millipore water purification system had the minimum resistivity of 18.0 MΩ cm. Argon and nitrogen gas were of ultra-purity grade. Silicon wafers with 0.56 mm thickness were purchased from University Wafer Company (Boston, MA) and cut into 12×6 mm^2 pieces.

2.2. Self-assembly of initiator monolayer on surface

Silicon wafers were treated first in a clean room environment before the grafting process. They were exposed to UV/ozone for 30 min, and then immersed in 0.15 M hydrofluoric acid solution for 20 min to remove silicon oxide layer. After that, they were rinsed thoroughly by deionized water, dried under a nitrogen stream, and exposed to UV/ozone again for 30 min to form a new contamination-free silicon oxide layer. The surface-attachable ATRP initiator, 6-(2-bromo-2-methyl) propionyloxy hexenyl trichlorosilane (BMPHTCS) was synthesized beforehand [51]. The pretreated silicon wafers were subsequently immersed in a 2.5 mM solution of BMPHTCS in dry toluene for 18 h at room temperature to form self-assembled initiator monolayers with thicknesses of 1.6 ± 0.2 nm. The surfaces were finally cleaned in toluene ultrasonically, rinsed 3 times, and then dried in an argon stream.

2.3. Preparation of POEGMA-b-PMETAC copolymer brushes on surface

To graft POEGMA brushes onto silicon wafers, $Cu^{I}Br$ (28.8 mg, 0.2 mmol) and Bipy (63.6 mg, 0.4 mmol) were first added to a 50-mL flask [33]. The flask was then evacuated and backfilled with argon 3 times to remove oxygen. Degassed OEGMA (12 g, 40 mmol) and methanol (20 mL) were then transferred into the flask. The solution was degassed with argon for another 30 min before it was transferred to a glove box filled with ultra-pure nitrogen. The free initiator EBIB (29.4 μL, 0.2 mmol) was added to the solution to initiate polymerization. After stirred for another 30 s, the reaction mixture was allocated to small glass tubes containing initiator-grafted silicon wafers. The grafting reaction was stopped by adding a methanol solution of $Cu^{II}Br_2$/Bipy after a certain period of time. The POEGMA-grafted surfaces were cleaned ultrasonically in methanol for a certain period of time, rinsed thoroughly, dried in an argon stream, and measured by ellipsometer. No further reduction in the POEGMA layer thickness after successive cleaning steps suggested a complete removal of the physically adsorbed POEGMA chains. The surfaces were finally dried in an argon stream, ready for grafting the second block.

To graft PMETAC block onto POEGMA-grafted surfaces, $Cu^{I}Cl$ (89.1 mg, 0.9 mmol), $Cu^{II}Cl_2$ (24.2 mg, 0.18 mmol) and Bipy (337.3 mmg, 2.16 mmol) were first placed into a 50-mL flask. It was evacuated and backfilled with argon for 3 times. Degassed METAC solution (10 g, 36 mmol METAC), methanol (10 mL) and water (2.5 mL) were then added to the flask. The mixture was degassed for another hour, then transferred to a glove box, distributed into small glass tubes with POEGMA-grafted silicon wafers. The grafting process was carried out at room temperature for a preset period of time and stopped by adding a methanol/water (volume ratio of 2:1) solution of $Cu^{II}Cl_2$/Bipy. The same cleaning procedure as described above was followed.

2.4. Characterization

The thickness of the grafts on the silicon wafers was measured by an ellipsometer (Exacta 2000, Waterloo Digital Electronics,

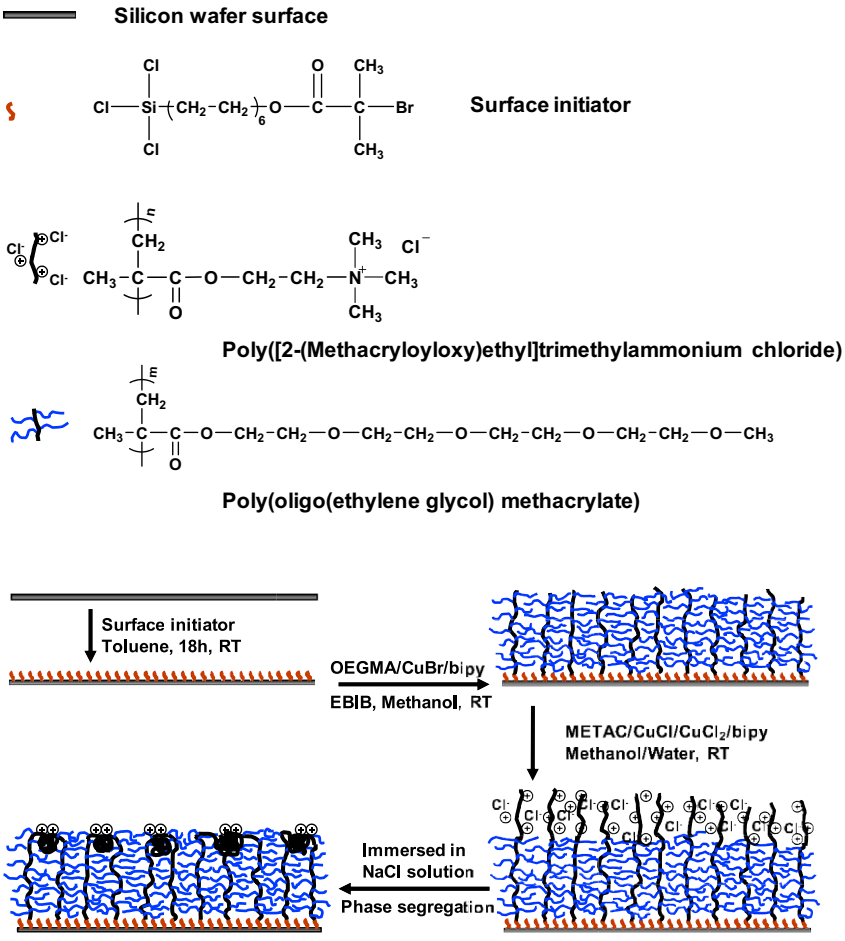

Scheme 1. Synthesis procedure for POEGMA-b-PMETAC copolymer brushes on silicon wafer via surface-initiated ATRP.

He–Ne laser (632.8 nm), incident angle 70°). The water contact angle was measured with a contact angle goniometer (Model 200, Rame-Hart instrument Co.). A NanoScope IIIa Multimode atomic force microscope (Digital Instruments, Inc.) was employed to observe surface morphology in air.

2.5. Protein adsorption experiments

Protein adsorption experiments were carried out in isotonic tris buffered saline (TBS) with radioiodinated fibrinogen. Fibrinogen is an important protein in blood plasma which is essential in blood coagulation. It has a molecular weight of 340,000 g/mol and a structure containing two sets of three different polypeptide chains, which are linked to each other by disulfide bonds [52]. It was selected as the model protein in this work because it has a large size and narrow dimension of 450 × 90 × 90 Å^3, which makes it detectable by AFM method. Its adsorption behavior on POEGMA surfaces was evaluated in our previous work [53]. To count the amount of protein adsorption on the surface, fibrinogen was radiolabeled with Na125I via the iodine monochloride (ICl) method [54]. Ion exchange chromatography was employed to remove unbound radioactive iodide. The solutions for protein adsorption contained only 10% radiolabeled proteins. The surfaces were immersed in the protein solution for 2 h allowing protein adsorption to reach equilibrium. The surfaces were then put into fresh TBS solution for 5 min (3 cycles) to remove loosely adsorbed proteins, dried and measured by a Wizard 3″ 1480 Automatic Gamma Counter (Perkin–Elmer Life Sciences) to count the amount of proteins adsorbed on the surface. For surface morphology observation by AFM method, the same procedure was used except that regular fibrinogen without radio labelling was used.

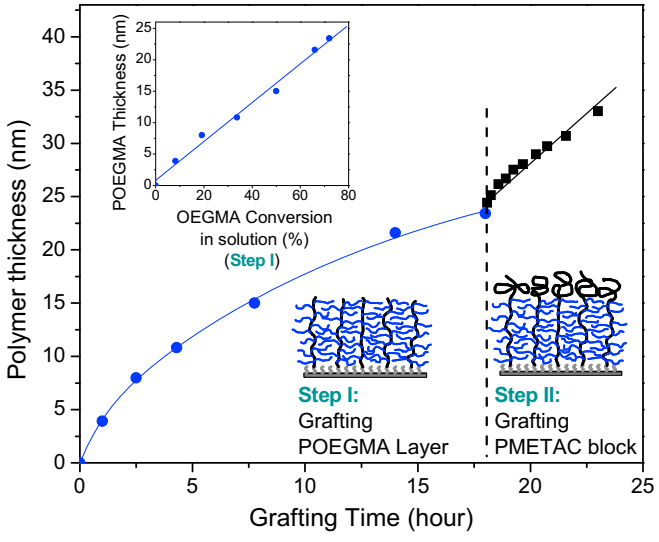

Fig. 1. Development of polymer graft thickness on silicon wafer. The thickness data are repeated with an error less than 5%.

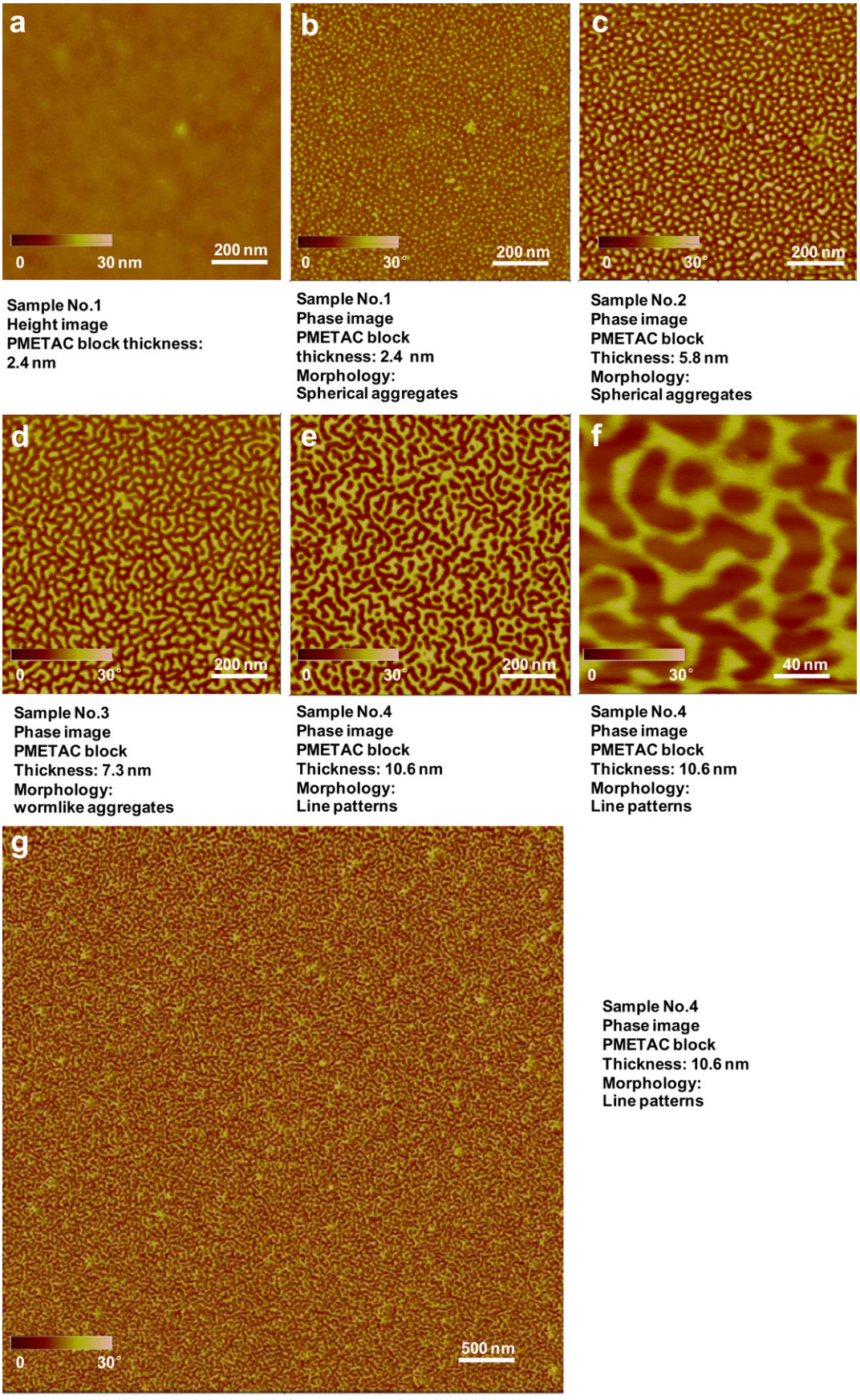

Fig. 2. AFM image of surface in air. All the samples have the same POEGMA layer thickness of 23.4 nm. PMETAC block varies from 2.4 nm to 10.6 nm.

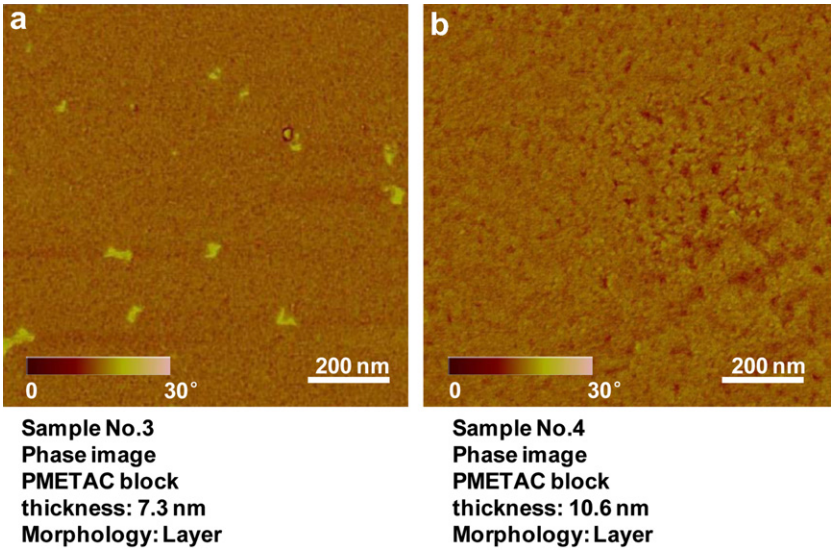

Fig. 3. AFM images after water treatment.

3. Results and discussion

3.1. Preparation of POEGMA-b-PMETAC copolymer brushes

The surface grafting procedure is described briefly in Scheme 1. After the pre-treatment of silicon wafers in a clean room, an initiator monolayer was grafted onto the surface. The surface-initiated ATRP of OEGMA was subsequently carried out at room temperature. The free initiator was added to the solution to generate deactivator and thus to assure the living character of ATRP. As shown in Fig. 1, the thickness of POEGMA brushes grow linearly with OEGMA conversion in the solution, demonstrating the living character of this system. The grafting process was stopped after 18 h at 72% conversion to minimize chain termination. The surfaces were cleaned ultrasonically in methanol and rinsed thoroughly to remove physically adsorbed POEGMA chains. The resulting POEGMA brushes had a thickness of 23.4 nm. The grafting density was estimated from the equation of $\Gamma = d\rho/M_n$, where d is the layer thickness, ρ is the polymer bulk density, and M_n is the polymer molecular weight, respectively. The molecular weight of grafted POEGMA cannot be measured directly, so it was assumed the molecular weight of grafted POEGMA was the same as that of free POEGMA in solution. It was measured by gel permeation chromatography. The estimated grafting density was 0.26 chains/nm^2 [51].

PMETAC block was grafted to the brushes through ATRP chain extension of POEGMA. The chain ends of the POEGMA brushes were reactivated by the catalyst in solution to initiate PMETAC grafting. Excess deactivator, instead of free initiator, was added to facilitate the living character of ATRP, especially in the early stage. As shown in Fig. 1, the thickness of the PMETAC block increased linearly with time, indicating a living grafting process [55,56]. Surfaces having PMETAC block thicknesses varying from 2.4 to 10.6 nm were prepared by controlling the grafting time. The chain length and polydispersity of grafted polymer chains on surface are difficult to be measured by experimental methods. In this work, the formation of different patterns and their ability to pattern proteins are discussed based on the variation in block thickness, which can be measured accurately by ellipsometer.

3.2. Formation of nanoscale patterns

The surfaces were immersed in a 0.5 mol/L NaCl solution for 4 h at room temperature, and were then dried in an argon flow (ultra-purity grade) for ~2 min. The dry state surface morphologies were observed by AFM, as shown in Fig. 2. Fig. 2(a) and (b) give the height

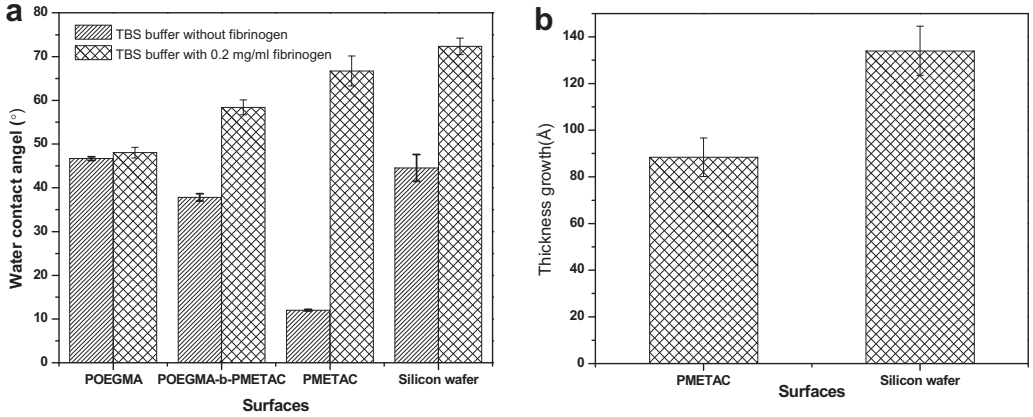

Fig. 4. (a) Water contact angle of the surfaces before and after fibrinogen adsorption. The advancing water contact angle was measured by the sessile drop method. (b) The increase in thickness on the surfaces after fibrinogen adsorption.

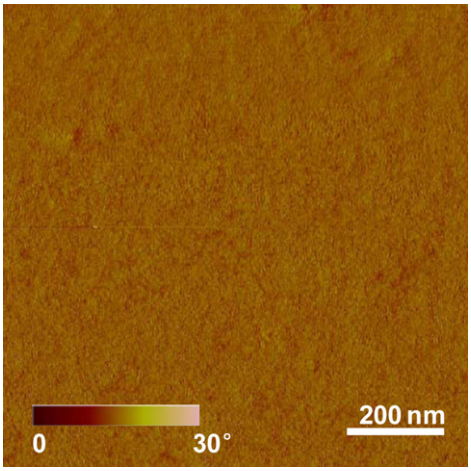

Fig. 5. AFM phase image of fibrinogen adsorption on the PMETAC surface.

and phase images of the same surface. The height image gives the height variation on the surface. The obtained patterned surface was still flat, as shown in Fig. 2(a). The phase image detects the chemical variation on the surface. Fig. 2(b) shows the patterns developed from the phase segregation between POEGMA and PMETAC. In the NaCl solution, PMETAC, a strong polyelectrolyte, collapsed on the POEGMA surface and thus formed nanoscale aggregates. The bright domains denote PMETAC, while the dark areas correspond to POEGMA. The chemical variations on the surface were targeted in this work; therefore only phase images were examined in details.

In the current study, the bottom POEGMA layer thickness was fixed to ~23.4 nm and the upper PMETAC layer thickness was varied from 2 nm to 12.0 nm. Different nanoscale patterns were achieved through varying PMETAC layer thickness. Our experimental observations showed qualitative similarity with the theoretical morphologies simulated by Shi et al. [57]. Their simulation work showed that the self-assembly of densely grafted block copolymer brushes could give a range of patterns including spherical aggregate, wormlike and line pattern etc. on the surface when the upper block thickness was varied.

Sample 1 and Sample 2 had the PMETAC layer thickness less than 6 nm, forming spherical aggregates as shown in Fig. 2(b) and (c). The smallest PMETAC domain size was less than 10 nm. In our previous work, the smallest domain size achieved by the self-assembly of POEGMA-block-PMMA brushes was 6–9 nm. These feature sizes are among the smallest ones achieved by the self-assembly of block copolymers, which normally gives feature sizes between 10 and 100 nm [16,18]. We believe that the long side chains of POEGMA effectively isolated the PMETAC aggregates and resulted in the small feature sizes.

When the PMETAC layer thickness was further increased, the spherical aggregates increased in size until they came into contact with each other forming the wormlike aggregates. As shown in Fig. 2(d), the wormlike aggregates formed when the PMETAC layer thickness was 7.3 nm. When the PMETAC layer thickness was increased to 10.6 nm, the PMETAC domains coalesced, forming a line pattern (Fig. 2(e)). In our studies, no parallel lines were achieved as described in Shi's simulation. External aids (e.g. pre-patterned substrates, electric field, mechanical flow field, temperature gradient etc) may help form the long-range regular patterns via the self-assembly method.

Fig. 2(f) gives a scan area of 200 nm × 200 nm to closely examine the line pattern. It is evident that the feature size is quite uniform, although the self-assembly method can only give random patterns. These random patterns with the uniform feature size can be employed as modules to prepare nanoscale products where only a random nanoscale structure is required, e.g. nanoscale membranes, nanoparticles and nanofibers, and high-efficient catalysis.

The advantage of the self-assembly method lies in its ability to prepare large area patterns at low costs. Fig. 2(g) gives a scan of 5 μm × 5 μm area. As it can be seen, no defects are observed. The feature size is very uniform in the large area.

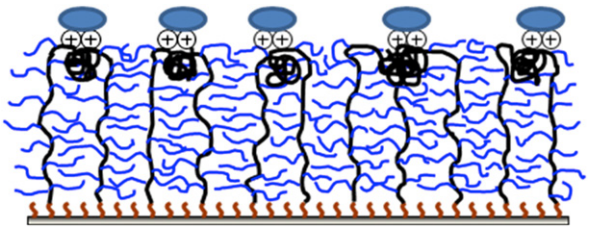

Scheme 2. The fibrinogen adsorption scheme on POEGMA-b-PMETAC nanopatterns.

3.3. Stimuli-responsive behavior

The nanoscale patterns formed after the surfaces were treated with NaCl solution. When the surfaces were treated with pure water, the PMETAC blocks stretched out from the surface, giving a complete PMETAC overlayer. Fig. 3(a) and (b) show the surface morphologies of Sample 3 and Sample 4 after the water treatment. The bright dots in Fig. 3(a) were caused by AFM tip contaminations. This switch of the surface morphologies was reversible through the treatment with different solvents. The overlayer morphology was observed in the samples having PMETAC thickness greater than 7 nm after treated with water. The overlayers in Sample 1 and Sample 2 were incomplete, because the PMETAC layers were too thin.

3.4. Protein adsorption on nanoscale patterns

The surfaces grafted with POEGMA brushes have been widely studied for their biocompatibility in resisting protein adsorption. It was found in our previous work that the surfaces grafted with POEGMA brushes adsorbed only 26 ng/cm^2 fibrinogen. Compared to the unmodified silicon wafer of 773 ng/cm^2, it was about 95% reduction. Fig. 4(a) shows the water contact angle measurements. The water contact angle of the POEGMA surface did not change significantly before and after fibrinogen adsorption. However, the water contact angle of silicon wafer surface was increased from 40° to 70° after the fibrinogen adsorption. The monolayer adsorption of fibrinogen on a flat surface is estimated to be between 140 and 700 ng/cm^2. The adsorption amount of 773 ng/cm^2 on silicon wafer indicates a complete coverage. The ellipsometry could not detect any increase in thickness of the POEGMA surface after fibrinogen adsorption. However, an increase of 13 nm in thickness was detected on silicon wafer after the fibrinogen adsorption, as shown in Fig. 4(b). The measurements confirmed the excellent performance of POEGMA brushes in resisting fibrinogen adsorption. In contrast, PMETAC could adsorb proteins through electronic interactions. Fig. 4(b) shows an increase of 8 nm thickness, suggesting adsorption of fibrinogen on the surface grafted with PMETAC brushes. The water contact angle changed from 10° to 70°, close to the typical value of a complete coverage of fibrinogen. The radio labelling experiment gave 240 ng/cm^2 fibrinogen adsorbed on the PMETAC surface. Fig. 5 shows the AFM image of a homogeneous surface after the fibrinogen adsorption, suggesting a complete coverage of fibrinogen on the PMETAC surface. All these results confirmed a monolayer of fibrinogen on the PMETAC surface.

Based on the above fibrinogen adsorption behaviour on POEGMA and PMETAC brushes, it was hypothesized that the

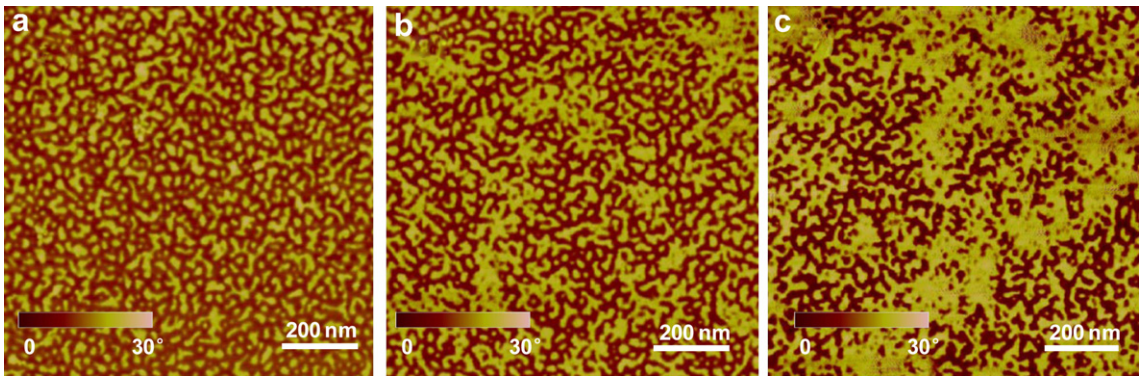

Fig. 6. AFM phase image of fibrinogen on POEGMA-b-PMETAC nanopatterns after protein adsorption with different fibrinogen concentrations: (a) 0.02 mg/mL, (b) 0.2 mg/mL and (c) 1 mg/mL.

nanopatterns prepared in this work from POEGMA-b-PMETAC have the ability to pattern proteins. As illustrated in Scheme 2, the PMETAC aggregates attract fibrinogen, while the POEGMA background repels the protein. A protein pattern similar to the original polymer pattern would form.

The protein concentration in solution is an important factor that determines the amount of protein adsorption on the surface. Three levels of concentration were studied in this work. A careful examination of three images in Fig. 6 reveals that fibrinogen was preferably adsorbed on PMETAC with an increase in the protein concentration. The contrast between PMETAC domains and POEGMA background increased obviously while the fibrinogen concentration was increased from 0.02 mg/mL (Fig. 6(a)) to 0.2 mg/mL (Fig. 6(b)). It is well known that fibrinogen tends to aggregate easily. It is evident in Fig. 6(b) that some fibrinogen aggregated and even covered a part of the POEGMA background. The aggregated fibrinogen has the exactly same color as the PMETAC domains, suggesting a complete coverage of the PMETAC domains by fibrinogen at 0.2 mg/mL. When the fibrinogen concentration was further increased to 1 mg/mL, more fibrinogen aggregated and started to cover the POEGMA background. It becomes clear that there exists an optimal fibrinogen concentration (about 0.2 mg/mL) for a complete coverage of the PMETAC domains but leaving POEMGA background clean. As shown in Fig. 4(a), the water contact angle of POEGMA-b-PMETAC surface after the protein adsorption at 0.2 mg/mL was 60°, between POEGMA (45°) and surfaces covered completely by fibrinogen (70°).

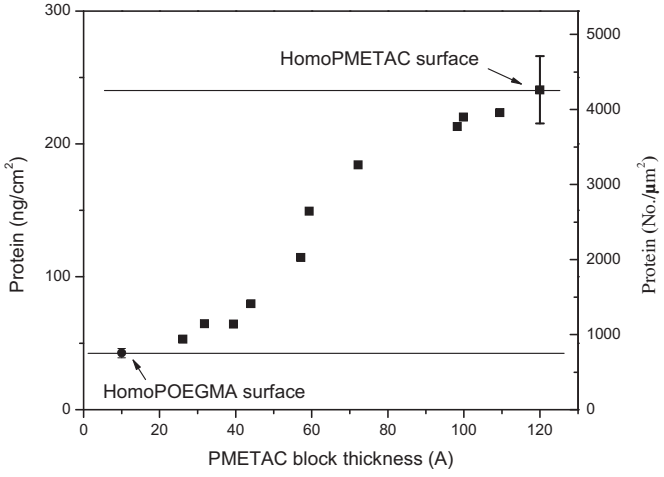

Fig. 7. The fibrinogen adsorption on POEGMA-b-PMETAC nanopatterns with different PMETAC block thickness.

The protein adsorption on the surface was also studied quantitatively by the radio labelling method. With the increase of the PMETAC block thickness, the PMETAC composition on the surface increased. The amount of adsorbed fibrinogen was expected to increase as well. The fibrinogen adsorption on the POEGMA-b-PMETAC nanopatterns with different PMETAC block thicknesses was studied at the optimal fibrinogen concentration of 0.2 mg/mL which enabled fibrinogen to give a complete coverage of the PMETAC domains but to leave the POEMGA background clean. As shown in Fig. 7, the amount of absorbed fibrinogen increased from a value close to that of POEGMA to that of PMETAC, as expected. When the PMETAC block thickness was between 5 nm and 10 nm, a quick increase was observed. Fig. 2 shows that during this range the patterns experienced the change in pattern type from spherical aggregates to wormlike aggregates, and then line patterns, suggesting an important role played by the pattern type in determining the amount of protein adsorption on the surface.

4. Conclusions

Various nanopatterns have been introduced through the self-assembly of grafted block copolymer brushes having two hydrophilic components. The design of two hydrophilic components was to avoid hydrophobic areas where proteins could change their conformations and lose their activity. The polyelectrolyte collapsed in salt solutions and induced phase segregation between the two hydrophilic blocks. The nanopatterns including spherical aggregates, wormlike aggregates and line patterns were obtained by simple adjustment of the thickness of upper block layer. The long side chains of POEGMA brushes helped constrain the feature size to about 10 nm and fine tune the size on a nanoscale. These patterns were reversibly switchable through treatments with selective solvents.

The behavior of fibrinogen adsorption on these patterns was studied by ellipsometry, water contact angle, AFM and radio labelling experiment. The results showed that PMETAC aggregates attracted fibrinogen while the POEGMA background repelled the protein. The polymer nanopatterns prepared in this work possessed the ability to pattern proteins. Protein patterns identical to the original polymer patterns were introduced with a proper level of the protein concentration.

Acknowledgments

The authors thank the Natural Sciences and Engineering Research Council of Canada (NSERC) for its financial support for this work and the Canada Foundation of Innovation (CFI) for some facilities.

References

[1] az-Mochon JJ, Tourniaire G, Bradley M. Chem Soc Rev 2007;36(3):449–57.
[2] Fink J, Thery M, Azioune A, Dupont R, Chatelain F, Bornens M, et al. Lab Chip 2007;7(6):672–80.
[3] Kane RS, Takayama S, Ostuni E, Ingber DE, Whitesides GM. Biomaterials 1999;20(23–24):2363–76.
[4] Blawas AS, Reichert WM. Biomaterials 1998;19(7–9):595–609.
[5] Falconnet D, Csucs G, Grandin HM, Textor M. Biomaterials 2006;27 (16):3044–63.
[6] Otsuka H, Nagasaki Y, Kataoka K. Curr Opin Colloid Interface Sci 2001;6(1):3–10.
[7] Senaratne W, Andruzzi L, Ober CK. Biomacromolecules 2005;6(5):2427–48.
[8] Rosi NL, Mirkin CA. Chem Rev 2005;105(4):1547–62.
[9] Blattler T, Huwiler C, Ochsner M, Stadler B, Solak H, Voros J, et al. J Nanosci Nanotechnol 2006;6(8):2237–64.
[10] Whitesides GM, Ostuni E, Takayama S, Jiang XY, Ingber DE. Annu Rev Biomed Eng 2001;3:335–73.
[11] Khademhosseini A, Bettinger C, Karp JM, Yeh J, Ling YB, Borenstein J, et al. J Biomater Sci-Polym Ed 2006;17(11):1221–40.
[12] Galaev IY, Mattiasson B. Trends Biotechnol 1999;17(8):335–40.
[13] Craighead HG, James CD, Turner AMP. Curr Opin Solid State Mat Sci 2001;5 (2–3):177–84.
[14] Shim J, Bersano-Begey TF, Zhu XY, Tkaczyk AH, Linderman JJ, Takayama S. Curr Top Med Chem 2003;3(6):687–703.
[15] Cheng JY, Ross CA, Smith HI, Thomas EL. Adv Mater 2006;18(19):2505–21.
[16] Geissler M, Xia YN. Adv Mater 2004;16(15):1249–69.
[17] Stoykovich MP, Nealey PF. Mater Today 2006;9(9):20–9.
[18] Krausch G, Magerle R. Adv Mater 2002;14(21):1579–83.
[19] Zhao B, Brittain WJ. J Am Chem Soc 1999;121(14):3557–8.
[20] Minko S, Muller M, Motornov M, Nitschke M, Grundke K, Stamm M. J Am Chem Soc 2003;125(13):3896–900.
[21] Xu C, Wu T, Drain CM, Batteas JD, Fasolka MJ, Beers KL. Macromolecules 2006;39(9):3359–64.
[22] Minko S. Polym Rev 2006;46(4):397–420.
[23] Zhou F, Huck WTS. Phys Chem Chem Phys 2006;8(33):3815–23.
[24] Luzinov I, Minko S, Tsukruk VV. Prog Polym Sci 2004;29(7):635–98.
[25] Zhao B, Brittain WJ, Zhou WS, Cheng SZD. J Am Chem Soc 2000;122 (10):2407–8.
[26] Tomlinson MR, Genzer J. Langmuir 2005;21(25):11552–5.
[27] Zhulina EB, Singh C, Balazs AC. Macromolecules 1996;29(19):6338–48.
[28] Prokhorova SA, Kopyshev A, Ramakrishnan A, Zhang H, Ruhe J. Nanotechnology 2003;14(10):1098–108.
[29] Santer S, Ruhe J. Polymer 2004;45(25):8279–97.
[30] Tomlinson MR, Genzer J. Polymer 2008;49(22):4837–45.
[31] Kong B, Lee JK, Choi IS. Langmuir 2007;23(12):6761–5.
[32] Huang WX, Kim JB, Baker GL, Bruening ML. Nanotechnology 2003;14 (10):1075–80.
[33] Gao X, Feng W, Zhu SP, Sheardown H, Brash JL. Langmuir 2008;24 (15):8303–8.
[34] Gao X, Kucerka N, Nieh MP, Katsaras J, Zhu SP, Brash JL, et al. Langmuir 2009;25(17):10271–8.
[35] Ma HW, Hyun JH, Stiller P, Chilkoti A. Adv Mater 2004;16(4):338–41.
[36] Lutz JF, Andrieu J, Uzgun S, Rudolph C, Agarwal S. Macromolecules 2007;40 (24):8540–3.
[37] Revzin A, Tompkins RG, Toner M. Langmuir 2003;19(23):9855–62.
[38] Lee BS, Lee JK, Kim WJ, Jung YH, Sim SJ, Lee J, et al. Biomacromolecules 2007;8 (2):744–9.
[39] Houseman BT, Huh JH, Kron SJ, Mrksich M. Nat Biotechnol 2002;20(3):270–4.
[40] Lee KB, Park SJ, Mirkin CA, Smith JC, Mrksich M. Science 2002;295 (5560):1702–5.
[41] Bruckbauer A, Zhou DJ, Kang DJ, Korchev YE, Abell C, Klenerman D. J Am Chem Soc 2004;126(21):6508–9.
[42] Falconnet D, Pasqui D, Park S, Eckert R, Schift H, Gobrecht J, et al. Nano Lett 2004;4(10):1909–14.
[43] Suh KY, Seong J, Khademhosseini A, Laibinis PE, Langer R. Biomaterials 2004;25(3):557–63.
[44] Smith JC, Lee KB, Wang Q, Finn MG, Johnson JE, Mrksich M, et al. Nano Lett 2003;3(7):883–6.
[45] Ichino M, Nagasaki Y. J Photopolym Sci Technol 2006;19(4):451–4.
[46] Lopez GP, Albers MW, Schreiber SL, Carroll R, Peralta E, Whitesides GM. J Am Chem Soc 1993;115(13):5877–8.
[47] Qian XP, Metallo SJ, Choi IS, Wu HK, Liang MN, Whitesides GM. Anal Chem 2002;74(8):1805–10.
[48] Csucs G, Michel R, Lussi JW, Textor M, Danuser G. Biomaterials 2003;24 (10):1713–20.
[49] Khademhosseini A, Jon S, Suh KY, Tran TNT, Eng G, Yeh J, et al. Adv Mater 2003;15(23):1995–2000.
[50] Khademhosseini A, Suh KY, Jon S, Eng G, Yeh J, Chen GJ, et al. Anal Chem 2004;76(13):3675–81.
[51] Feng W, Chen RX, Brash JL, Zhu SP. Macromol Rapid Commun 2005;26 (17):1383–8.
[52] Fuss C, Palmaz JC, Sprague EA. J Vasc Interv Radiol 2001;12(6):677–82.
[53] Feng W, Zhu SP, Ishihara K, Brash JL. Langmuir 2005;21(13):5980–7.
[54] Archambault JG, Brash JL. Colloid Surf B-Biointerfaces 2004;33(2):111–20.
[55] Ramakrishnan A, Dhamodharan R, Ruhe J. Macromol Rapid Commun 2002;23 (10–11):612–6.
[56] Ramakrishnan A, Dhamodharan R, Ruhe J. J Polym Sci Pol Chem 2006;44 (5):1758–69.
[57] Yin YH, Sun PC, Li BH, Chen TH, Jin QH, Ding DT, et al. Macromolecules 2007;40(14):5161–70.